

# Submicron size single crystal $\text{Me}^{\text{IV}}\text{B}_2$ (Me = Ti, Zr, Hf) fibers

Yuriy B. Paderno<sup>a,\*</sup>, Vladimir B. Filipov<sup>a</sup>, Varvara N. Paderno<sup>a</sup>, Ali Sayir<sup>b</sup>

<sup>a</sup> I. Frantsevich Institute for Problems of Materials Sciences of Academy of Sciences of NASU, 3 Krzhizhanovsky str., Kiev 03142, Ukraine

<sup>b</sup> NASA Glenn Research Center and Case Western Reserve University, Cleveland, OH, USA

Available online 4 February 2005

## Abstract

Submicron diameter  $\text{ZrB}_2$ ,  $\text{TiB}_2$  and  $\text{HfB}_2$  fibers were produced in single crystal form. Directional solidification of diboride eutectics followed by matrix phase removal was utilized to fabricate single crystal fibers.  $\text{LaB}_6$  was utilized as the matrix phase for crystal growth. Fiber diameter ranged from 0.4 to 0.8  $\mu\text{m}$  for all compositions investigated. The length-to diameter aspect ratio exceeded 500 for all compositions. Fibers were uniform and had smooth surfaces along the entire length. Transmission electron microscopy characterization showed that the fibers were single crystals with a high degree of perfection and preferential growth direction along the (1 1 1) orientation of the diboride lattice. Porous structures were formed by pressing the diboride fibers and sintering at temperatures up to 2200 K in vacuum. The level of porosity, average pore size distribution, and specific surface area could be controlled to some extent by mechanical pressing. The diborides in small fiber form may have technical applications in structural components and functional devices, i.e., industrial filters, thermal protection systems, and possibly for reinforcement.

© 2005 Elsevier Ltd. All rights reserved.

**Keywords:** Grain growth; Fibres; Permeability; Borides; Refractories

## 1. Introduction

A considerable amount of information has been accumulated over the years about metal carbides, nitrides and silicides. In contrast to silicides and carbides, the borides have not been studied adequately due to lack of processing techniques. Specifically, the diborides of the group IVB to VIB transition metals has not been studied adequately in single crystal form and is the subject of this investigation. The analysis of physical, mechanical and chemical properties of the group IVB–VIB diborides<sup>1–6</sup> has shown that they may well be one of the most advanced materials. The most representative compound of the diborides is the zirconium diboride ( $\text{ZrB}_2$ ). Zirconium diboride has a very high melting temperature ( $\sim 3500$  K) and exhibits high chemical stability, particularly in some metal matrices such as steel and cast iron. In addition,  $\text{ZrB}_2$  has a high elastic modulus ( $\sim 500$  GPa) and retains its strength at elevated temperatures. The intrinsic properties of the group IVB–VIB diborides has not been adequately char-

acterized due to lack of good quality single crystals. Single crystal fibers have potential for applications for structural components and functional devices, i.e., industrial filters, thermal protection systems, and high strength composites.

Small diameter fibers, in single-crystal form, are desirable because their strength can approach theoretical values.<sup>1–5</sup> Whiskers of titanium, zirconium, niobium diborides have been produced by chemical vapor deposition (CVD). CVD utilizes the reaction of appropriate metal chlorides and boron in hydrogen containing atmosphere.<sup>7,8</sup> Short whiskers have been produced by CVD but they are not adequate for structural applications. CVD has been successful fabricating thick coatings<sup>9</sup> but has not been successful in fabricating high aspect ratio (length/diameter) fibers. CVD utilizing a vapor–liquid–gas phase reaction requires catalytic metallic inclusions that are difficult to remove and consequently deteriorates high temperature properties. Several other methods, i.e., the melt, extrusion, centrifuging of fusion, sol–gel processing, and pyrolysis<sup>1–5</sup> are not feasible for the production of diboride compounds due to unfavorable thermodynamic conditions.

The present study investigated the microstructural properties of sub-micron fibers of  $\text{ZrB}_2$ ,  $\text{TiB}_2$  and  $\text{HfB}_2$  produced by

\* Corresponding author. Tel.: +38 0 44 424 13 67; fax: +38 0 44 444 31 21.

E-mail address: [paderno@ipms.kiev.ua](mailto:paderno@ipms.kiev.ua) (Y.B. Paderno).

directional solidification of eutectics (DSE). The single crystals were grown in a  $\text{LaB}_6$  matrix and the fibers were extracted by dissolution of the  $\text{LaB}_6$ . This approach is related to solution growth of metal diboride crystals using metal solution-melts.<sup>10</sup> However, fibers are produced by DSE instead of platelet shaped crystals.

## 2. Experimental

The composites consisting of  $\text{LaB}_6$  matrix phase and  $\text{ZrB}_2$ ,  $\text{TiB}_2$  and  $\text{HfB}_2$  fibers were fabricated using DSE mixtures of the corresponding boride phases. Sintered rods of the eutectic compositions were melted using RF heating. Directional solidification was carried out utilizing the float zone technique. The experimental details of this process have been previously published<sup>11</sup> and will not be repeated again. The removal of the diboride fibers was performed by dissolving of  $\text{LaB}_6$  matrix in a dilute nitric acid solution; the duration of dissolution was determined by dimension of eutectic rods and temperature, usually was 10–15 min.

Characterization of the fibers was done by X-ray diffraction (XRD), scanning electron microscopy (SEM) and transmission electron microscopy (TEM). The crystallographic orientation, resolved by TEM (Hitachi HU-200F), along the fiber length was determined by using thin foils of the DSE samples. TEM dark field image analysis was also used utilized to characterize the single crystal fibers. Stereo-Scan S4-10 SEM was used to study the microstructures. Fiber permeability measurements were done using mercury injection porosimeter (Pore-Sizer 9300 by Micromeritics, USA).

## 3. Results and discussion

Binary eutectic alloys can form regular structures during directional solidification under certain conditions. The formation of regular or irregular phases depends on the crystallography of each phase. The orientation relationship of the coincident interface between the phases has a strong influ-

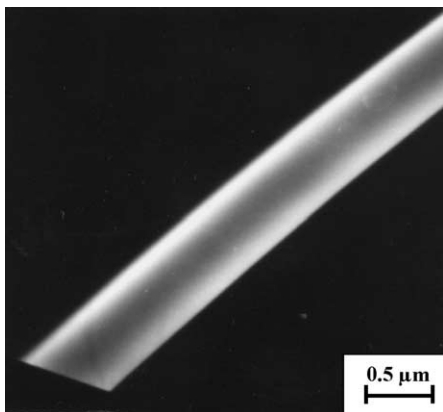


Fig. 1. Unit threadlike crystal of the zirconium diboride.

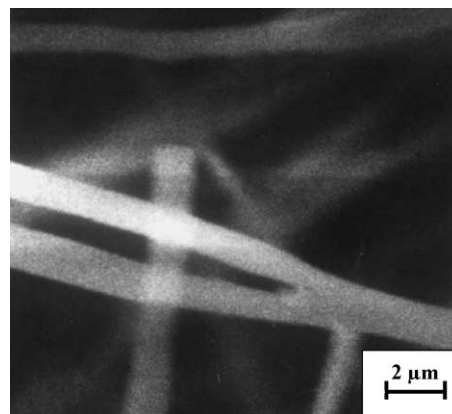


Fig. 2. The area of growth imperfection in the threadlike crystal of zirconium diboride.

ence. In addition to the intrinsic crystallographic properties, the temperature gradient and solidification rate influences the structure. The boride eutectics of transition and rare-earth metals form a regular structure during solidification due to the specific crystallographic relationship. The transition metal diboride phase forms a regular array of submicron size fibers in a metal hexaboride phase.<sup>11–15</sup> We used the eutectic solidification theory to optimize the structure of the  $\text{LaB}_6$ – $\text{ZrB}_2$ ,  $\text{LaB}_6$ – $\text{HfB}_2$  and  $\text{LaB}_6$ – $\text{TiB}_2$  eutectics as a means to produce single crystal fibers of  $\text{ZrB}_2$ ,  $\text{TiB}_2$  and  $\text{HfB}_2$ .

The  $\text{ZrB}_2$ ,  $\text{TiB}_2$  and  $\text{HfB}_2$  fibers were removed from  $\text{LaB}_6$  phase using acid etching and washing. The typical representative SEM micrograph of  $\text{ZrB}_2$  fiber is shown in Fig. 1. The fiber maintains its uniformity along the length and has a very smooth surface. The fiber diameter for all transition metal diborides ( $\text{TiB}_2$ ,  $\text{ZrB}_2$  and  $\text{HfB}_2$ ) was extremely small ranging between 0.4 and 0.8  $\mu\text{m}$ , controlled mainly by  $\text{MeB}_2$  type and the solidification rate. The diameter of the  $\text{TiB}_2$  and  $\text{HfB}_2$  fibers was 0.8 and 0.4  $\mu\text{m}$ , respectively. The length of such crystals was usually determined by distribution of strain field distortions during crystallization that causes the branching of

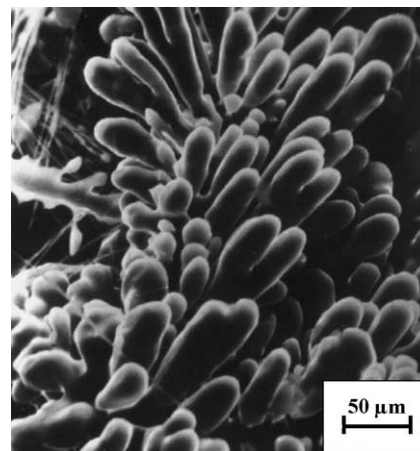


Fig. 3. Configuration of solidified  $\text{ZrB}_2$  phase obtained by the shifted from the optimal conditions.

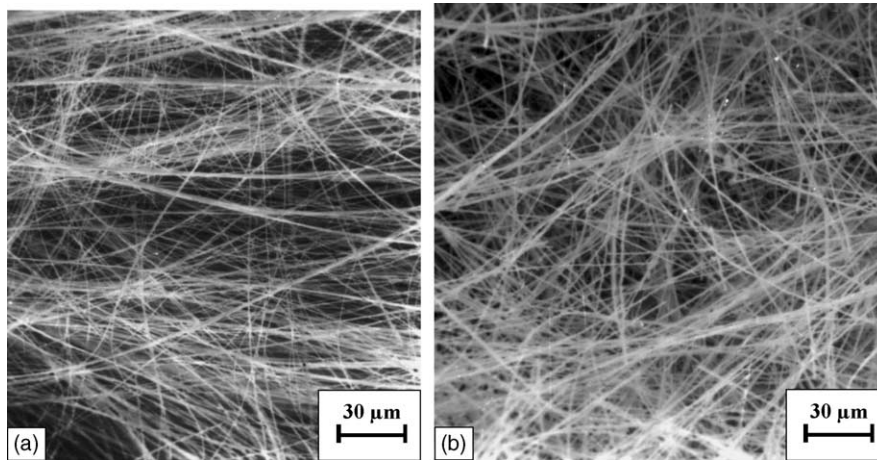


Fig. 4. The zirconium (a) and hafnium (b) diborides threadlike crystals.

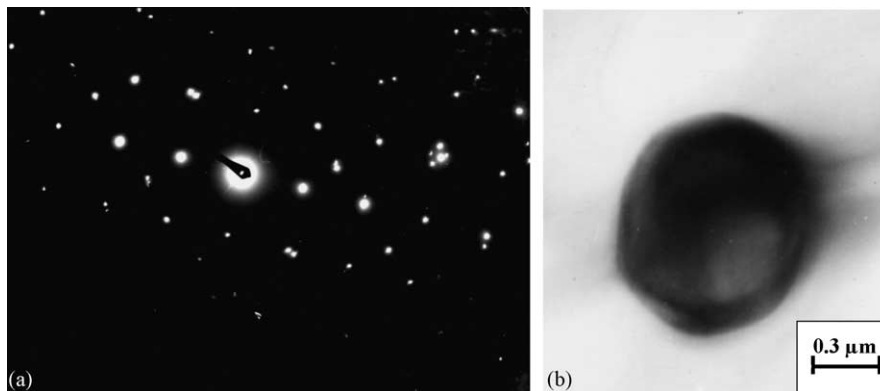


Fig. 5. Electron diffraction pattern (a) and transverse cross-section of the threadlike crystal (b) inside of the  $\text{LaB}_6$  matrix (thin foil method).

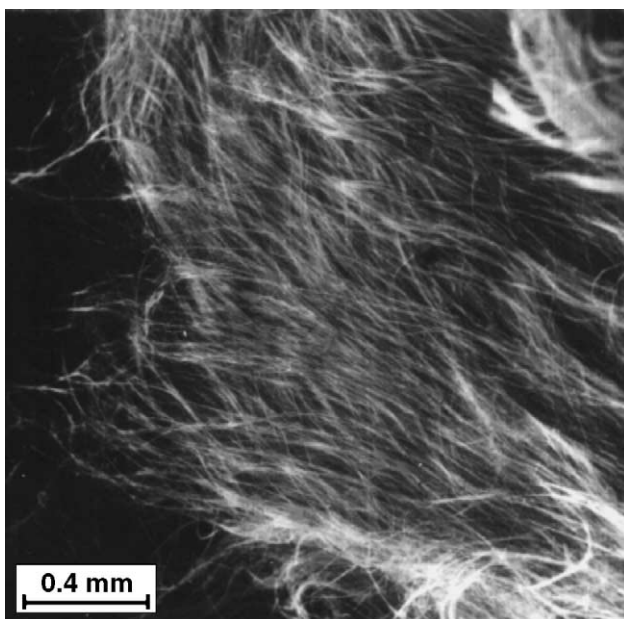


Fig. 6. Feltlike view of the zirconium diboride threadlike crystals.

the phases as shown in Fig. 2. For all systems studied,  $\text{TiB}_2$ ,  $\text{ZrB}_2$  and  $\text{HfB}_2$ , the length-to-diameter aspect ratio was 500 or higher.

The solidification of the  $\text{LaB}_6\text{--Me}^{\text{IV}}\text{B}_2$  systems produced a regular array of polyphase structure. The spatial distribution of the phases and their volume fraction were determined by the composition at the eutectic invariant point. The deviation from the eutectic composition of the melt distorts the heat flow distribution during the solidification and did affect the microstructure. The  $\text{ZrB}_2$  phase morphology obtained by the solidification of the off-eutectic composition and very slow speed of crystallization are shown in Fig. 3. Initiation of several branches and an increase of the diameter are apparent to accommodate the compositional changes.

The prerequisite to achieve uniform structures was related to the intimate mixing of the starting compositions to minimize any departure from the eutectic composition. The tight control of the solidification parameters required a steep temperature gradient and rigorous control of the processing temperature. These conditions facilitated the formation of regular structures and subsequently production of very uniform diameter diboride fibers. Fig. 4 shows representative SEM micrograph of uniform small diameter  $\text{ZrB}_2$  and  $\text{HfB}_2$  fibers.



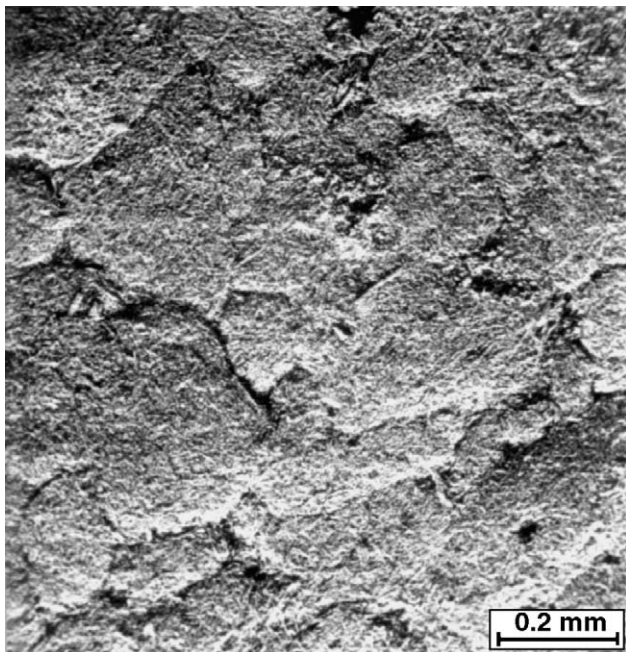


Fig. 7. View of the porous  $ZrB_2$  elements pressed by 50 MPa, sintered at  $1900^\circ C$ .

The diboride fibers were single crystal as determined by the electron diffraction pattern analysis (Fig. 5a) and growth preferentially in  $[0001]$  direction. The transverse cross-section of the DSE samples crystals exhibits a near perfect hexagonally ordered array of fibers (Fig. 5b). Further examination of crystal structure and degree of perfection was completed using the dark-field image analysis<sup>16</sup> (Fig. 1). The Bragg's reflections (diffraction contrast) did not have any divergence at the analyzed sections of samples suggesting a high degree of perfection of the crystal structure. The absence of any measurable diffraction contrast in small diameter crystals indicated that these fibers might have superior properties.

As mentioned previously, the diboride fibers may be suitable for different permeable components. Single crystal di-

boride fibers formed a continuous network and behave like a felt without any additional treatment, Fig. 6. The mechanical integrity of the felt was very high and permitted strong handling. The strength of the felt was related to number of contacts that fibers formed with each other. The number of contacts for the individual fibers was several orders of magnitude higher than those of inter-particles bonds of an ideal powder compact of the same density. The vast amount of fiber-to-fiber contacts formed an interlocking network that constructed a mechanically strong felt.

The felts made from  $MeB_2$  ( $Me = Ti, Zr, Hf$ ) fibers offer unique control of the porosity range. Fiber felts were compacted uniaxially at 10–120 MPa at room temperature and sintered at 1800–2200 K in vacuum. A representative SEM micrograph of a felt pressed at 50 MPa and sintered at 1900 K is shown in Fig. 7. The relative distribution of pore sizes is shown in Fig. 8 for different compact pressures. The specific surface area, porosity and average pore diameter for different processing conditions are summarized in Table 1. The porosity, specific surface area and average pore diameter monotonically decreased with increasing applied pressure. It is noteworthy to point out that pore diameter distribution was narrower at the low-pressure range of 10–20 MPa. The distribution characteristics (marked 3–5 in Fig. 8) did not change with increasing pressure above 30 MPa, presumably due to high elastic moduli of the fibers.

Table 1

Some characteristics of the pressed and sintered ( $T = 1900^\circ C$ ) permeable elements made from the  $ZrB_2$  threadlike single crystals

#	Pressure (MPa)	Porosity (%)	Specific surface		Average porous diameter ( $\mu m$ )
			$m^2/g$	$m^2/cm^3$	
1	10	84.30	0.899	0.872	3.2
2	20	74.60	0.577	0.903	2.5
3	40	60.74	0.419	1.02	1.6
4	80	48.70	0.330	1.05	1.3
5	120	49.2 <sup>a</sup>	0.400	1.25	1.25

<sup>a</sup> The porosity was increased due to the stratification of the pressed sample.

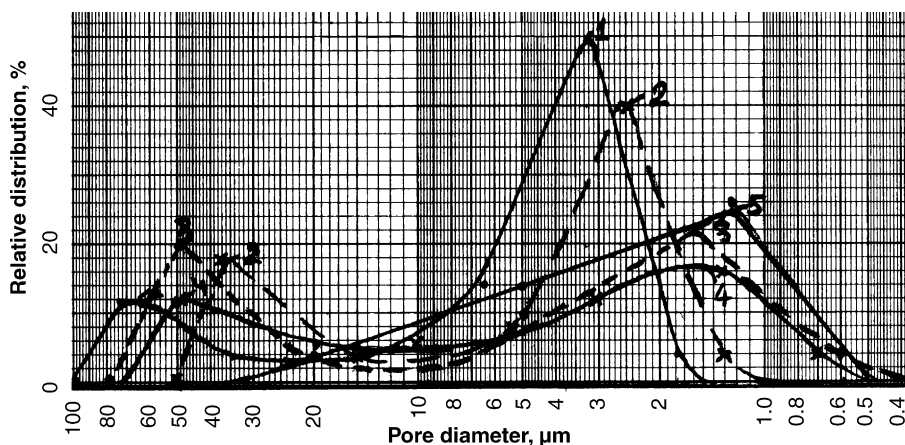


Fig. 8. Integral pore diameter distribution in the permeable elements pointed in Table 1.

#### 4. Summary

Single crystal fibers of  $ZrB_2$ ,  $HfB_2$  and  $TiB_2$  have been produced from the  $LaB_6$ – $ZrB_2$ ,  $LaB_6$ – $HfB_2$  and  $LaB_6$ – $TiB_2$  directionally solidified eutectic systems. Fiber extraction was performed by removal of the  $LaB_6$  matrix phase. Preferential growth direction of the single crystal fibers was the  $(0001)$  orientation for all compositions. The fibers contained no defects and had a high degree of perfection as determined by dark field image analysis. Fiber diameters were 0.4–0.8  $\mu\text{m}$  and their length-to-diameter aspect ratio exceeded 500.

The technological significance of the  $MeB_2$  ( $Me = \text{Ti, Zr, Hf}$ ) fiber has been demonstrated by fabrication of fiber felts with specific pore size characteristics. Superior thermal and chemical stability of  $MeB_2$  compounds and narrow fiber diameter distribution offer unique opportunity to fabricate porous structures that may find applications in thermal protection systems, transpiration, filtration of corrosive melts and possible as a reinforcement of structural composites.

#### References

1. Levitt, A. P., ed., *Whisker Technology*. Wiley-Interscience, New York, London, Sydney, Toronto, 1970.
2. Hertzberg, R. B., Directional crystallization of eutectic alloys for creation of reinforced composites. In *Fiber Composite Materials*, ed. W. Hibbard, American Society for Metals, Metals Park, OH, 1965, pp. 99–109.
3. Karol-Porzynski, C. Z., *Advanced Materials. Refractory Fiber and Fibrous Metals Composites*. Astex Publ. Comp. LTD, Guilford, 1962.
4. Broutman, L. J. and Krock, R. H., ed., *Modern Composite Materials*. Addison-Wesley Publ. Comp, Massachusetts, 1967.
5. Frantsevich, I. N., ed., *Composite Materials of Fibrous Structure*. Naukova Dumka, Kiev, 1970 (in Russian).
6. Kosolapova, T. Y. a., ed., *Properties, Preparation and Application of Refractory Compounds, Handbook*. Metallurgiya, Moscow, 1986 (in Russian).
7. Motojima, S. and Sugiyama, K., Chemical vapor growth of  $Cr_5Si_3$  whiskers and hollow crystals. *J. Cryst. Growth*, 1981, **55**(3), 611–615.
8. Motojima, S., Sugiyama, K. and Takahashi, Y., Chemical vapor deposition of niobium ( $NbB_2$ ). *J. Cryst. Growth*, 1975, **30**, 233–239.
9. Sayir, A., Carbon fiber reinforced hafnium carbide composite. *J. Mater. Sci.*, 2004, **39**, 5995–6003.
10. Nakano, K., Hajashi, H. and Imura, T., Single crystal growth of IVa-diborides from metal solutions. *J. Cryst. Growth*, 1974, **24–25**, 679–682.
11. Paderno, Yu., Paderno, V. and Filippov, V., Some peculiarities of structure formation in eutectic d- and f-transition metals boride alloys. In *Boron-Rich Solids, AIP Conference Proceedings, Vol 231*, eds. D. Emin, T. L. Aselage, A. C. Switendick, B. Morosin and C. L. Beckel, 1991, pp. 561–569.
12. Paderno, Yu., Paderno, V. and Filippov, V., Crystal chemistry of eutectic growth of d- and f-transition metals borides. *Jpn. J. Appl. Phys., Series*, 1994, **10**, 190–193.
13. Paderno, Yu., Paderno, V. and Filippov, V., Some crystal chemistry relationships in eutectic cocrystallization of d- and f-transition metal borides. *J. Alloys Compd.*, 1995, **219**, 116–118.
14. Paderno, Yu., Paderno, V. and Filippov, V., Some peculiarities of eutectic crystallization of  $LaB_6$ – $(Ti,Zr)B_2$  alloys. *Solid State Chem.*, 2000, **154**, 165–167.
15. Paderno, Yu., Paderno, V., Shitsevalova, N. and Filippov, V., The peculiarities of the structure formation in directionally crystallized eutectics  $EuB_6$ – $MB_2$ . *J. Alloys Compd.*, 2001, **317–318**, 367–371.
16. Hirsch, P. B., Howie, A., Nicholson, R. B., Pashley, D. W. and Whelan, M. J., *Electron Microscopy of Thin Crystals*. Butterworths, London, 1965.